

RBFNN-HOMS Nonsingular Terminal Sliding Control of n -DOF Robotic Manipulator

Amar Rezoug*, **Bertrand Tondu****, **Mustapha Hamerlain***, **Mohamed Tadjine*****

**DRP, Centre de Développement des Technologies Avancées, Baba Hassen 16303, Algiers, Algeria (Tel: +213555450740, e-mail: arezoug@cda.dz).*

*** INSA-LAAS, Groupe GEPETTO, Pôle RIA, 135 Avenue de Ranguil 31077, Toulouse, France (bertrand.tondu@insa-toulouse.fr).*

****PCL, Automatic Control Department, polytechnic national school Algiers, Algeria (tadjine@yahoo.fr).*

Abstract: Hybridization of the Sliding Mode Control schemes and the Artificial Intelligence techniques is a relatively new way in the control research domain. This paper proposes a robust control scheme by the adoption of Non-singular Terminal Sliding Mode Control (NTSMC), Higher Order Sliding Mode (HOSM) and Neural Network (NN) structure for n -DOF robotic manipulator. The NTSMC is used with Time Delay Estimation (TDE) method where the equivalent control term is synthesized without requirement of the robot model. In order to overcome the chattering drawback of the NTSMC, the discontinuous term is replaced by an adaptive HOSM controller. The adaptive HOSM controller consists of the Super Twisting algorithm (STW) which is estimated adaptively using Radial Based Function Neural Network (RBFNN) structure. The used RBFNN is learned online without requirement of a prior knowledge of training data. The stability is proved using a candidate Lyapunov function and the controller parameters are adjusted adaptively. The superiority and the effectiveness of the proposed approach are tested with a Three Degree of Freedom (3-DOF) Robot Manipulator (RM) in trajectory tracking task and compared with STW.

Keywords: Terminal Sliding Mode Control, Super Twisting Algorithm, Radial Based Function Neural Networks, Time Delay Estimation, Robot Manipulator, Lyapunov Stability.

1. INTRODUCTION

During the last decades, Robotic Manipulators (RM) have been widely considered in both academic and industrial fields owing to some superior advantages such as higher accuracy and stiffness, speed trajectory tracking and so on (Van et al., 2013; Jin et al., 2013; Rezoug et al., 2013; Jin et al., 2009; Jin et al., 2011). However, these systems contain large structured and unstructured inherent uncertainties which may even cause instability. Due to such effects, performances and robustness of linear controllers used for these systems are very limited. To overcome the shortcomings of linear controllers, several nonlinear controllers have been proposed such as feedback linearization (Kuo et al., 1989), adaptive control (Pazelli et al., 2012), computed torque control (Lewis et al., 2004), model predictive control (Song et al., 1999), sliding mode control (Mondal et al., 2014; Kumar et al., 2014), and many others.

Sliding Mode Control (SMC) is well known as nonlinear and naturally robust method which is suitable for controlling systems in presence of measurement errors, parametric variations and external disturbances (Perruquetti, 2002). SMC can be subdivided into two main classes. The first class is the traditional SMC called First Order SMC (FSMC). The fact that FSMC generates the chattering phenomenon, a second class called Higher Order Sliding Mode control (HOSM) has been proposed (Levant, 1993). Some HOSMs

have been applied to RM such as: Twisting in (Perruquetti, 2002), Super-Twisting (Lei et al., 2014) and Sub-Optimal (Capisania et al., 2009). However, these approaches are very sensitive to the noise effects and can only reduce the chattering. Terminal Sliding Mode Control (TSMC) is a particular case of HOSM which can be used also as a FSMC (Mondal et al., 2014; Rezoug et al., 2011). This technique has been studied for further improving the control performance, particularly, for achieving best finite time convergence. The Non-singular Terminal Sliding Mode Control (NTSMC) based on the RM model is given in (Fenga et al., 2002) this approach takes into account the robot parametric uncertainties. Since the exact models of the robotic systems and the aforementioned bounds of the controller parameters' are not always obtainable in practice which makes this approach to be complicated to implement. In (Jin et al., 2009) the authors propose a NTSMC approach incorporated into a Time Delay Estimation (TDE) method for RM trajectory tracking task where the objective is to compensate the nonlinear terms and uncertainties in RM dynamics. However, the higher control part is replaced by saturation function that reduces the performances and the robustness.

On the other hand, Neural Networks (NN) schemes are among the approaches usually used in order to estimate and/or to control systems which contain uncertain dynamics (Tang et al., 2006, Lu et al., 2010; Kumar et al., 2014). Traditional back propagation NN is characterized by the

inconveniences of slow learning and local minimal convergence. The Radial Based Neural Network (RBFNN) is a particular type of feed-forward NN, which contains only a single hidden layer of neurons usually characterized by Gaussian Activation Functions (GAF) (rezoug et al, 2012). Since RBFNN can be used without requirement of a training data, we can consider it as the best candidate to solve the classical NN problems.

To the best of authors' knowledge, the hybridizations of the FSMC, HOSM and artificial intelligence techniques are proposed and applied to RM only in (Manceur et al., 2012; Van et al., 2013,). Manceur et al., (Manceur et al., 2012) proposed the hybridization of FSMC, STW and type-2 fuzzy logic system for controlling single-input single-output nonlinear system. The authors have successfully applied their approach under a real One Degree of Freedom (1-DOF) RM. However, the use of type-2 fuzzy logic requires a sophisticated and fast data processing system which is not always available. Recently, Van et al., have been proposed a Takagi-Sugeno (T-S) fuzzy second-order sliding mode observer-controller (Van et al., 2013). This approach preserves the advantages of the both techniques, such as the low online computational burden of the T-S fuzzy model, low chattering, fast response and finite time convergence of the second-order sliding mode. The stability and convergence of the proposed closed loop observer-based controller strategy is proven by a Lyapunov method. However, T-S fuzzy model reduces the mathematical description of the robotic system and, consequently, the performances and the robustness.

In this paper, we propose a new robust control approach for n -DOF RM. This controller consists of the combination of NTSMC, STW controller and RBFNNs which is named RBFNN-Super-Twisting Non Singular Terminal Sliding Mode Control (NNSTW). The NTSMC is used with TDE method where the equivalent control term is synthesized without requirement of the robot model. In order to overcome the chattering drawback caused by the NTSMC, the discontinuous term is replaced by STW. In order to remove the chattering effect, RBFNNs are used to estimate the two terms of the STW. Stability of the robot in close loop is guaranteed using Lyapunov theorem. The proposed control scheme allows us (1) To avoid the nonlinear modelling problems, (2) To guarantee the stability and the robustness of the robot (3) To eliminate the chattering effects and (4) To improve the speed convergence of the state space variables.

This paper is organized as follow: In Section 2, the RM model and the NTSMC based on the TDE method are presented. In Section 3, the proposed NNSTW for n -DOF RM is designed. In order to show the proposed control scheme superiority and effectiveness, the simulation experiments in trajectory tracking are performed in Section 4. Finally, in Section 5, the paper is surmised by a conclusion.

2. PRELIMINARY

The RM dynamic model and its control using NTSMC based on the TDE method presented in this section.

2.1. n -DOF robot manipulator model:

The standard form of an n -DOF RM dynamic model is given as:

$$M(q)\ddot{q} + C(q, \dot{q})\dot{q} + G(q) + F(q, \dot{q}) + \tau_d = \tau \quad (1)$$

Where:

- $M(q) \in \mathbb{R}^{n \times n}$ is the inertial matrix which is symmetric positive non-singular and bounded by $m_{\min} \|x\|^2 \leq x^T Mx \leq m_{\max} \|x\|^2 \quad \forall x \in \mathbb{R}^n$, with m_{\max} and m_{\min} are minimum and maximum eigenvalues of $M(q)$.
- $C(q, \dot{q}) \in \mathbb{R}^{n \times n}$ is the matrix of centrifugal and coriolis terms.
- $G(q) \in \mathbb{R}^{n \times 1}$ is the vector of gravitational force.
- $F(q, \dot{q}) \in \mathbb{R}^{n \times 1}$ is the vector of friction.
- $q \in \mathbb{R}^{n \times 1}$, $\dot{q} \in \mathbb{R}^{n \times 1}$ and $\ddot{q} \in \mathbb{R}^{n \times 1}$ are the position, the velocity and the acceleration vectors, respectively.
- $\tau \in \mathbb{R}^n$ is the torque input vector.
- $\tau_d \in \mathbb{R}^{n \times 1}$ is the vector of generalized input due to the disturbances (such as an added payload, etc.) , with $\|\tau_d\| < \beta_d$, and β_d is a positive real value.

2.2. Non-Singular Terminal Sliding Mode Control based on the TDE

In the design of TSMC for a RM, the control objective is to drive the joint position q to the desired position q_d in finite time. As in conventional SMC, the TSMC requires to define the sliding variable. Then, conventional Terminal Sliding Variable (TSV) (S) is given as:

$$S = \dot{e} + \Lambda e^p \quad (2)$$

Where: $e = q - q_d$ and $\dot{e} = \dot{q} - \dot{q}_d$ with q_d and \dot{q}_d are the desired trajectory vectors and theirs time derivatives, respectively.

$\rho = q/p$, with p and q are constants odd integers with $p > q$. Then, ρ is a real positive constant.

$\Lambda = \text{diag}(\lambda_{ii}) > 0$ is a diagonal matrix with λ_{ii} are real positive values and ($i=1 \dots n$).

The use of the TSV (equation 2) will generate the so-called singularity problem. This problem resides in the division by zero which appeared in the general form of the TSMC. In order to overcome this drawback, we have adopted the NTSMC which was firstly proposed in (Fenga et al., 2002). In NTSMC, the TSV is modified as follows:

$$S = e + \Lambda^{-1} \dot{e}^\gamma \quad (3)$$

Where: $1 < \gamma = \rho^{-1} = \frac{p}{q} < 2$ (Fenga et al., 2002).

Let us consider now the diagonal matrix $\bar{M} = \text{diag}(m_{ii})$ with m_{ii} are positive real constants. Substituting \bar{M} in (1), the n -DOF RM dynamics can be rewritten as (Jin et. al 2009, Youcef-Toumi et al., 1989):

$$\bar{M}\ddot{q} + N(q, \dot{q}, \ddot{q}) = \tau \quad (4)$$

Where:

$$N(q, \dot{q}, \ddot{q}) = [M(q) - \bar{M}]\ddot{q} + C(q, \dot{q})\dot{q} + G(q) + F(q, \dot{q}) + \tau_d$$

At the instant $t-L$, $N(q, \dot{q}, \ddot{q})_{t-L}$ can be obtained from (4) as:

$$N(q, \dot{q}, \ddot{q})_{t-L} = \tau_{t-L} - \bar{M}\ddot{q}_{t-L} \quad (5)$$

Where: L is chosen usually as the sampling time.

By using the principle of the TDE $N(q, \dot{q}, \ddot{q})_{t-L}$ is given as:

$$N(q, \dot{q}, \ddot{q})_{t-L} = \hat{N}(q, \dot{q}, \ddot{q}) \quad (6)$$

Where: $\hat{N}(q, \dot{q}, \ddot{q})$ is the estimation of $N(q, \dot{q}, \ddot{q})$ at $t-L$. This assumption is available only if L is sufficiently fast.

The extraction of \ddot{q} from the time derivative of TSV (equation) made equal to zero ($\dot{S} = 0$) and its substituting in equation (4) yields:

$$\tau = \bar{M}[\ddot{q}_d + \gamma^{-1}\Lambda\dot{e}^{2-\gamma}] + \hat{N}(q, \dot{q}, \ddot{q}) \quad (7)$$

According to equation (6) we can rewrite equation (7) as:

$$\tau = \bar{M}[\ddot{q}_d + \gamma^{-1}\Lambda\dot{e}^{2-\gamma}] + N(q, \dot{q}, \ddot{q})_{t-L} \quad (8)$$

By replacing equation (5) in (8), we can write the NTSMC based on the TDE as:

$$\tau = \tau_{t-L} + \bar{M}[\ddot{q}_d - \ddot{q}_{t-L} + \gamma^{-1}\Lambda\dot{e}^{2-\gamma} + U] \quad (9)$$

With:

$$U = -K_{sw}\text{Sign}(S) \quad (10)$$

Where: U is the discontinuous control part.

3. PROPOSED CONTROLLER

This section is composed of two subsections. In the Subsection 3.1 Non-singular Terminal Super Twisting controller for n -DOF RM is proposed where the Super Twisting is used as a solution to reduce the chattering drawback. While in the Subsection 3.2 the estimation of the super twisting controller parts using the RBFNN is proposed. Stability analysis and the new controller parameters adjustment are also detailed in this subsection.

3.1. Non-singular Terminal Super Twisting Control

In order to overcome NTSMC drawback (the chattering caused by $-K_{sw}\text{Sign}(S)$ (equation 10)), we have opted to use the HOSM controller. Among the HOSM controller most used is the STW. This last is developed and analysed for controlling only systems having relative degree equal to one

with respect to the input. The STW law consists of adding two terms (Shtessel et al., 2014, Levant, 2003), which has the nonlinear PI profile (equation 11). The advantage of the STW consists of its dependence only of the sliding variable compared with twisting and sub-optimal algorithms which are depended on the sliding variable derivatives. The STW algorithm for n -DOF RM can be written as:

$$U = -\beta|S|^{1/2}\text{sign}(S) - \alpha\int_0^{t_c}\text{sign}(S)dt \quad (11)$$

Where: $\beta = \text{diag}(\beta_i) \in \mathbb{R}^{n \times n}$ and $\alpha = \text{diag}(\alpha_i) \in \mathbb{R}^{n \times n}$ are positive diagonal matrices, t_c is the convergence time such as the controlled system converged in the neighborhood of v , with v is defined as (Manceur et al., 2012):

$$|S| \leq v \quad (12)$$

With:

$$t_c = \begin{cases} t & \text{if } |S| > v \\ t_v & \text{if } |S| \leq v \end{cases} \quad (13)$$

As t_c is unknown previously, we set $t=0$ then $t_c = t$ until $|S|=v$. Then, t_c takes the value of t corresponding to the instant when $|S|=v$.

Then, at $t=t_c$ equation (11) is substituted by:

$$U = -\beta|S|^{1/2}\text{sign}(S) - \alpha \cdot t_c \cdot \text{sign}(S) \quad (14)$$

The optimal control law (U^*) of (14) is given as:

$$U^* = -\beta^*|S|^{1/2}\text{sign}(S) - \alpha^* \cdot t_c \cdot \text{sign}(S) \quad (15)$$

Where: $\beta^* = \text{diag}(\beta_{ii}^*) \in \mathbb{R}^{n \times n}$ and $\alpha^* = \text{diag}(\alpha_{ii}^*) \in \mathbb{R}^{n \times n}$ are diagonal matrices with positive optimal values.

The positive control of (15) can be written as:

$$|U^*| = \beta^*|S|^{1/2} + \alpha^* \cdot t_c \quad (16)$$

Replacing equation (11) in the control law (9), we obtain a new control called nonsingular terminal STW controller as:

$$\tau = \tau_{t-L} + \bar{M} \left[\ddot{q}_d - \ddot{q}_{t-L} + \gamma \cdot \Lambda \dot{e}^{2-\gamma} - \beta|S|^{1/2}\text{sign}(S) - \alpha \int_0^{t_c}\text{sign}(S(\tau))d\tau \right] \quad (17)$$

The control law in equation (17) contains an integral discontinuous function which gives only chattering attenuation (Tang et al., 2006). In addition, STW is very sensitive to the noise effects. In order to improve the performance of the control and to eliminate the chattering drawback, we will replace the two terms of the STW controller by two RBFNNs for each joint. This proposition will be detailed in the Section 3.2.

3.2. Adaptive RBFNN Nonsingular Terminal Sliding HOMs Control

This section is composed of three subsections: First, the estimation of the STW parts using RBFNNs is given in a general form. Second, the used RBFNNs architectures are detailed. Third, stability analysis with RBFNNs parametric adjustment is presented.

A. Estimation of the STW Controller Using RBFNN

In the proposed approach two RBFNNs are used to estimate the discontinuous and the integral term of the STW control respectively, in this case, equation (11) is substituted by:

$$\tilde{U} = -U = \begin{bmatrix} |S|^{1/2} W_1^{1T} h_1^1(S) \text{Sign}(S_1) + W_1^{2T} h_1^2(S) \int_0^{t_{s1}} \text{Sign}(S_1) d\tau \\ \vdots \\ |S|^{1/2} W_n^{1T} h_n^1(S) \text{Sign}(S_n) + W_n^{2T} h_n^2(S) \int_0^{t_{sn}} \text{Sign}(S_n) d\tau \end{bmatrix} \quad (18)$$

Where: W_i^1 is the weight vector of the RBFNN used for the estimation of the first part of the STW controller for joint i . W_i^2 is the weight vector of the RBFNN used for the estimation of the second part of the STW controller for joint i . $h_i^1(S)$ is the Gaussian activation vector of the RBFNN used for the estimation of the first part of the STW for joint i . $h_i^2(S)$ is the Gaussian activation vector of the RBFNN used to estimate the second part of the STW for joint i .

By replacing U in equation (9) by (\tilde{U}) , we obtain the following control law:

$$\tau = \tau_{t-L} + \bar{M} \left[\ddot{q}_d - \ddot{q}_{t-L} + \gamma^{-1} \cdot \Lambda \cdot \dot{e} \cdot 2^{-\gamma} - \tilde{U} \right] \quad (19)$$

The proposed control (19) is called Radial Based Function Neural Network Nonsingular Terminal Sliding Super Twisting Controller (NNSTW). In the next section the architecture of the used RBFNNs will be detailed.

B. The RBFNNs Architecture

The RBFNN can generate a map between the input and the output with relatively large desired accuracy. This type of NN structure can estimate effectively large nonlinear dynamics (Lei et al., 2014). However, RBFNN can give a best estimation only with enough sampling data and time. In our case, in order to simplify the controller estimation, we have adopted the decentralized RBFNN architecture. Therefore, for each joint; we have used two RBFNN to estimate the two parts of the STW. It is very important to note that it is possible to use a Multi-Input and Multi-Output (MIMO) RBFNN for controlling a RM as reported in (Kumar et al., 2014; Lu et al., 2010). However, the use of this structure has some disadvantages. First, the complexity and the misunderstanding of the MIMO RBFNN dynamics increase more and more with the increase of the joints number to be controlled. Second, the computing time will be very important with the increase of the joints number. The

adjustment of the RBFNN MIMO parameters is delicate because it is required to find the best combination for several joints at the same time, etc.

The used RBFNN is composed of three layers as shown in the Figure 1. In order to take into account the coupling, the input layer contains the TSV of joint i and the TSV of joint $i+1$. The middle layer is called hidden layer which is composed of m neurons where each neuron is characterized by Gaussian Activation Functions (GAF). The output layer gives the estimation of the STW parts.

Each neuron of the hidden layer is characterized by GAF which is given by:

$$h_{ji}^1 = e^{-\left(\frac{\|X_{ji} - c_{ji}\|}{2\sigma_{ji}^2}\right)} \quad \text{and} \quad h_{ri}^2 = e^{-\left(\frac{\|X_{ri} - c_{ri}\|}{2\sigma_{ri}^2}\right)} \quad (20)$$

Where: c_{ji} and c_{ri} are the centers of the GAFs. $j=1\dots J$ and $r=1\dots R$, J and R are the RBFNNs sizes. σ_{ji} and σ_{ri} are the variances of the GAF, i is the number of joint.

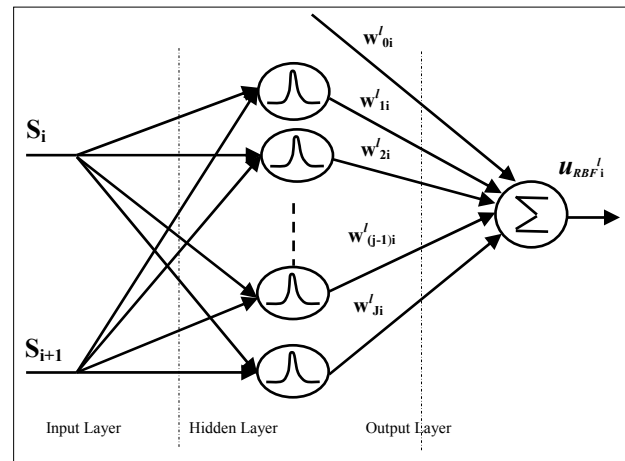


Fig. 1. Structure of the used RBFNNs for the estimation of the STW part with $l=\{1,2\}$, i is the number of joints, for the second control part j should be replaced by r .

The RBFNN output of joint i is computed by two terms as:

$$u_{RBFi}^1 = \sum_{j=1}^J w_{ji}^1 \times h_{ji}^1 = W_i^1 h_i^1 \quad (21)$$

$$u_{RBFi}^2 = \sum_{r=1}^R w_{ri}^2 \times h_{ri}^2 = W_i^2 h_i^2$$

Where: u_{RBFi}^1 and u_{RBFi}^2 are the estimated parts of the two terms of the STW for joint i . w_{ji}^1 and w_{ri}^2 are weights associated with the output for joint i . h_{ji}^1 and h_{ri}^2 are Gaussian functions. W_i^1 and W_i^2 are the weight vectors. The output of the neuron for given data is a radial function of the distance between the neuron center C_{ji} and C_{ri} and the sliding variables S for joint i and $i+1$ (Rezoug et al., 2012) while:

$$\begin{aligned}\|S-C_{ji}\| &= (S_i - c_{ji1})^2 + (S_{i+1} - c_{j(i+1)2})^2 \\ \|S-C_{ni}\| &= (S_i - c_{ni1})^2 + (S_{i+1} - c_{r(i+1)2})^2\end{aligned}\quad (22)$$

C. Stability Analysis and Parameters Adjustment of the NNSTW Controller

For the n -DOF RM controlled by the control law (19), we have chosen a candidate Lyapunov function as:

$$V = \frac{1}{2} S^T S + \sum_{i=1}^n \frac{1}{2\delta_i^1} \tilde{W}_i^{1T} \tilde{W}_i^1 + \sum_{i=1}^n \frac{1}{2\delta_i^2} \tilde{W}_i^{2T} \tilde{W}_i^2 \quad (23)$$

Where: δ_i^1 and δ_i^2 are positive real values for each joint i . $\tilde{W}_i^1 = W_i^1 - W_i^{1*}$ and $\tilde{W}_i^2 = W_i^2 - W_i^{2*}$. with W_i^{1*} and W_i^{2*} are the optimal weight vectors for each joint i .

The time derivative of equation (23) yields:

$$\dot{V} = S^T \dot{S} + \sum_{i=1}^n \frac{1}{\delta_i^1} \tilde{W}_i^{1T} \dot{W}_i^1 + \sum_{i=1}^n \frac{1}{\delta_i^2} \tilde{W}_i^{2T} \dot{W}_i^2 \quad (24)$$

The time derivative of the TSV (equation 3) is given by the following equation:

$$\dot{S} = \dot{e} + \gamma \Lambda^{-1} \text{diag}(e^{\gamma-1}) \ddot{e} \quad (25)$$

Substituting equation (11) in (25) we obtain:

$$\begin{aligned}\dot{S} &= \left\{ \dot{e} + \gamma \Lambda^{-1} \text{diag}(e^{1-\gamma}) \right. \\ &\quad \times \left[-\gamma \Lambda^{-1} \dot{e}^{2-\gamma} \left(-\beta |S|^{1/2} \text{sign}(S) - \alpha \int_0^t \text{sign}(S(\tau)) d\tau + \varepsilon \right) \right] \\ &\quad \left. = \gamma \Lambda^{-1} \dot{e}^{\gamma-1} \left(-\beta |S|^{1/2} \text{sign}(S) - \alpha \int_0^t \text{sign}(S(\tau)) d\tau + \varepsilon \right) \right\}\end{aligned}\quad (26)$$

Where: $\varepsilon = \hat{M}^{-1} (N - N_{i,r})$.

Replacing STW controller (equation 11) by the RBFNN given in equation (18), \dot{S} becomes:

$$\begin{aligned}\dot{S} &= \gamma \Lambda^{-1} \dot{e}^{\gamma-1} (-\tilde{U} + \varepsilon) \\ &= \gamma \Lambda^{-1} \dot{e}^{\gamma-1} \left(- \begin{bmatrix} |S|^{1/2} W_1^{1T} h_1^1(S) \text{Sign}(S_1) + W_1^{2T} h_1^2(S) \int_0^{t_1} \text{Sign}(S_1) d\tau \\ \vdots \\ |S|^{1/2} W_n^{1T} h_n^1(S) \text{Sign}(S_n) + W_n^{2T} h_n^2(S) \int_0^{t_n} \text{Sign}(S_n) d\tau \end{bmatrix} + \varepsilon \right)\end{aligned}\quad (27)$$

Let us denote:

$$\tilde{U}^* = \begin{bmatrix} |S_1|^{1/2} W_1^{1*T} h_1^1(S) \text{Sign}(S_1) + W_1^{2*T} h_1^2(S) \int_0^{t_1} \text{Sign}(S_1) d\tau \\ \vdots \\ |S_n|^{1/2} W_n^{1*T} h_n^1(S) \text{Sign}(S_n) + W_n^{2*T} h_n^2(S) \int_0^{t_n} \text{Sign}(S_n) d\tau \end{bmatrix} \quad (28)$$

Equation (28) is the optimal case of the equation (18). If we add and subtract \tilde{U}^* from the equation (27), it turns in \dot{S} :

$$\begin{aligned}\dot{S} &= \gamma \Lambda^{-1} \dot{e}^{\gamma-1} \left(- \begin{bmatrix} |S_1|^{1/2} (W_1^1 - W_1^{1*})^T h_1^1(S) \text{Sign}(S_1) + (W_1^2 - W_1^{2*})^T h_1^2(S) \int_0^{t_1} \text{Sign}(S_1) d\tau \\ \vdots \\ |S_n|^{1/2} (W_n^1 - W_n^{1*})^T h_n^1(S) \text{Sign}(S_n) + (W_n^2 - W_n^{2*})^T h_n^2(S) \int_0^{t_n} \text{Sign}(S_n) d\tau \end{bmatrix} \right. \\ &\quad \left. + (-\tilde{U}^* + \varepsilon) \right) \\ &= \gamma \Lambda^{-1} \dot{e}^{\gamma-1} \left(- \begin{bmatrix} |S_1|^{1/2} \tilde{W}_1^{1T} h_1^1(S) \text{Sign}(S_1) + \tilde{W}_1^{2T} h_1^2(S) \int_0^{t_1} \text{Sign}(S_1) d\tau \\ \vdots \\ |S_n|^{1/2} \tilde{W}_n^{1T} h_n^1(S) \text{Sign}(S_n) + \tilde{W}_n^{2T} h_n^2(S) \int_0^{t_n} \text{Sign}(S_n) d\tau \end{bmatrix} \right. \\ &\quad \left. - \tilde{U}^* + \varepsilon \right)\end{aligned}\quad (29)$$

Substituting equation (29) in (24) the time derivative of the Lyapunov function becomes:

$$\begin{aligned}\dot{V} &= S^T \left(\gamma \Lambda^{-1} \dot{e}^{\gamma-1} \left(- \begin{bmatrix} |S_1|^{1/2} \tilde{W}_1^{1T} h_1^1(S) \text{Sign}(S_1) + \tilde{W}_1^{2T} h_1^2(S) \int_0^{t_1} \text{Sign}(S_1) d\tau \\ \vdots \\ |S_n|^{1/2} \tilde{W}_n^{1T} h_n^1(S) \text{Sign}(S_n) + \tilde{W}_n^{2T} h_n^2(S) \int_0^{t_n} \text{Sign}(S_n) d\tau \end{bmatrix} \right) \right) \\ &\quad + S^T \gamma \Lambda^{-1} \dot{e}^{\gamma-1} (-\tilde{U}^* + \varepsilon) + \sum_{i=1}^n \frac{1}{\delta_i^1} \tilde{W}_i^{1T} \dot{W}_i^1 + \sum_{i=1}^n \frac{1}{\delta_i^2} \tilde{W}_i^{2T} \dot{W}_i^2 \\ &= S^T \left[\gamma \Lambda^{-1} \dot{e}^{\gamma-1} (-\tilde{U}^* + \varepsilon) \right] \\ &\quad + \gamma \Lambda^{-1} S^T \dot{e}^{\gamma-1} \left(- \begin{bmatrix} |S_1|^{1/2} \tilde{W}_1^{1T} h_1^1(S) \text{Sign}(S_1) + \tilde{W}_1^{2T} h_1^2(S) \int_0^{t_1} \text{Sign}(S_1) d\tau \\ \vdots \\ |S_n|^{1/2} \tilde{W}_n^{1T} h_n^1(S) \text{Sign}(S_n) + \tilde{W}_n^{2T} h_n^2(S) \int_0^{t_n} \text{Sign}(S_n) d\tau \end{bmatrix} \right) \\ &\quad + \sum_{i=1}^n \frac{1}{\delta_i^1} \tilde{W}_i^{1T} \dot{W}_i^1 + \sum_{i=1}^n \frac{1}{\delta_i^2} \tilde{W}_i^{2T} \dot{W}_i^2 \\ &= S^T \left[\gamma \Lambda^{-1} \dot{e}^{\gamma-1} (-\tilde{U}^* + \varepsilon) \right] \\ &\quad + \sum_{i=1}^n \tilde{W}_i^{1T} \left(\frac{1}{\delta_i^1} \dot{W}_i^1 - \gamma \lambda_i^{-1} \dot{e}_i^{\gamma-1} S_i |S_i|^{1/2} h_i^1(S) \text{Sign}(S_i) \right) \\ &\quad + \sum_{i=1}^n \tilde{W}_i^{2T} \left(\frac{1}{\delta_i^2} \dot{W}_i^2 - \gamma \lambda_i^{-1} \dot{e}_i^{\gamma-1} S_i h_i^2(S) \int_0^{t_i} \text{Sign}(S_i) d\tau \right)\end{aligned}\quad (30)$$

We take:

$$\begin{aligned}\dot{W}_i^1 &= \gamma \delta_i^1 \lambda_i^{-1} \dot{e}_i^{1-\gamma} S_i \|S\|^{3/2} h_i^1(S) \\ \dot{W}_i^2 &= \gamma \delta_i^2 \lambda_i^{-1} \dot{e}_i^{1-\gamma} h_i^2(S) \int_0^{t_i} |S_i| d\tau\end{aligned}\quad (31)$$

Using equation (31) the time derivative of the Lyapunov candidate function becomes:

$$\begin{aligned}\dot{V} &= S^T \left[\gamma \Lambda^{-1} \dot{e}^{\gamma-1} (-\tilde{U}^* + \varepsilon) \right] \\ &= \gamma \sum_{i=1}^n S_i \lambda_i^{-1} \dot{e}_i^{\gamma-1} \left(-(\tilde{u}_i^{1*} + \tilde{u}_i^{2*}) + \varepsilon_i \right)\end{aligned}\quad (32)$$

At $t=t_c$ and from (11) we can written (28) as:

$$\tilde{U}^* = \begin{bmatrix} \|S\|^{1/2} W_1^{1*T} h_1^1(S) + W_1^{2*T} h_1^2(S) t_{c1} \\ \vdots \\ \|S\|^{1/2} W_n^{1*T} h_n^1(S) + W_n^{2*T} h_n^2(S) t_{cn} \end{bmatrix} \times \text{diag}(\text{Sign}(S_i)) \quad (33)$$

Where:

$$\begin{aligned} \alpha_i^* &= W_i^{1*T} h_i^1(S) \\ \beta_i^* &= W_i^{2*T} h_i^2(S) \end{aligned} \quad (34)$$

From (33) we can write equation (32) as:

$$\dot{V} \leq \gamma \sum_{i=1}^n S_i \lambda_i^{-1} \dot{\epsilon}_i^{\gamma-1} \left(-\left(\|S_i\|^{1/2} W_i^{1*T} h_i^1(S) + W_i^{2*T} h_i^2(S) t_{ci} \right) \text{Sign}(S_i) + \epsilon_i \right) \quad (35)$$

Using equation (35) \dot{V} becomes:

$$\dot{V} = \gamma \sum_{i=1}^n \lambda_i^{-1} \dot{\epsilon}_i^{\gamma-1} \left(-\left(\beta_i^* |S_i|^{1/2} + \alpha_i^* t_{ci} \right) |S_i| + \epsilon_i S_i \right) \quad (36)$$

Because $\gamma = p/q > 0$, then, $\dot{\epsilon}_i^{\gamma-1} > 0$ and $\lambda_i^{-1} > 0$, we can guarantee \dot{V} negative if $\beta_i^* |S_i|^{1/2} + \alpha_i^* t_{ci} \geq \epsilon_i$, then, the stability of the controlled system is confirmed.

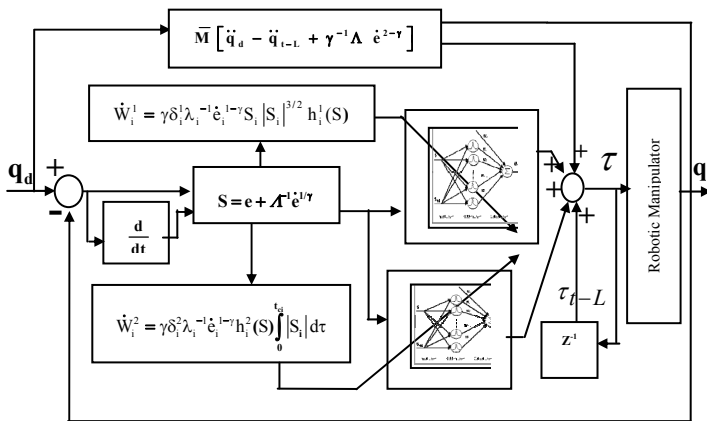


Fig. 2. NNSTW Control scheme.

The control system structure is composed of nominal control term and two STW estimated using RBFNNs as shown in Figure 2.

4. APPLICATION

In order to evaluate the proposed control approach, simulation experiments have been realized using 3-Degrees of Freedom (3-DOF) RM depicted in figure 3. The 3-DOF robot dynamic model is given by equation (37). The robot parameters based on (Gokhan et al., 2006) are given as:

$m_1 = 1 \text{ kg}$, $m_2 = 0.9 \text{ kg}$, $m_3 = 0.7 \text{ kg}$, $l_1 = 1 \text{ m}$, $l_2 = 0.8 \text{ m}$, $l_3 = 0.6 \text{ m}$ and $g = 9.8 \text{ m/sec}^2$.

During our experiments the trajectory tracking mode was adopted. Hence, all joints start from initial position equal to zeros $(q_{d1}(0), q_{d2}(0), q_{d3}(0)) = (0, 0, 0)$ and the objective is to

arrive to $(q_{d1}(10), q_{d2}(10), q_{d3}(10)) = (\frac{\pi}{4}, \frac{\pi}{4}, \frac{\pi}{4})$ through equation (38).

Simulations have been coded using MATLAB environment under the ODE45 solver. All joints are simulated for a time of 10 second with sampling time equal to 10ms. This sampling time is sufficient to compute in real time the proposed controller.

$$\begin{bmatrix} M_{11} & M_{12} & M_{13} \\ M_{21} & M_{22} & M_{23} \\ M_{31} & M_{32} & M_{33} \end{bmatrix} \begin{bmatrix} \ddot{q}_1 \\ \ddot{q}_2 \\ \ddot{q}_3 \end{bmatrix} + l_1 l_2 \sin(q_2) \begin{bmatrix} C_{11} & C_{12} & C_{13} \\ C_{21} & C_{22} & C_{23} \\ C_{31} & C_{32} & C_{33} \end{bmatrix} \begin{bmatrix} \dot{q}_1 \\ \dot{q}_2 \\ \dot{q}_3 \end{bmatrix} + \begin{bmatrix} 0 \\ 0 \\ -m_3 g \end{bmatrix} + F(\dot{q}) = \tau \quad (37)$$

Where:

$$\begin{aligned} M_{11} &= l_1^2 \left(\frac{m_1}{3} + m_2 + m_3 \right) \\ &\quad + l_1 l_2 (m_2 + 2m_3) \cos(q_2) + l_2^2 \left(\frac{m_2}{3} + m_3 \right) \\ M_{13} &= M_{23} = M_{31} = M_{32} = 0 \\ M_{12} &= M_{21} = -l_1 l_2 \left(\frac{m_2}{2} + m_3 \right) \cos(q_2) - l_2^2 \left(\frac{m_2}{3} + m_3 \right) \\ M_{22} &= -l_2^2 \left(\frac{m_2}{3} + m_3 \right) \\ M_{33} &= m_3 \\ C_{11} &= -\dot{q}_2 (m_2 + 2m_3) & C_{12} &= -\dot{q}_2 \left(\frac{m_2}{2} + m_3 \right) \\ C_{22} &= -\dot{q}_2 \left(\frac{m_2}{2} + m_3 \right) \\ C_{13} &= C_{22} = C_{23} = C_{31} = C_{32} = C_{33} = 0 \end{aligned}$$

$$F(\dot{q}) = \begin{bmatrix} 0.2 \text{Sign}(S_1) \\ 0.2 \text{Sign}(S_2) \\ 0.2 \text{Sign}(S_3) \end{bmatrix}$$

The common parameters of the two controllers (STW and NNSTW) for all joints are: $\bar{M} = \text{diag}(0.2, 0.2, 4)$, $q=5$, $p=7$ and $\Lambda = \text{diag}(0.7, 0.7, 0.2)$.

In the case of the STW we have the following parameters: $\alpha = \text{diag}(80, 90, 26.4)$ $\beta = \text{diag}(4.1, 40, 0.11)$. In the case of NNSTW controllers the used RBFNNs sizes are: RBFNN1 for joint 1 has 26 nodes, RBFNN 2 for joint 1 has 28 nodes, RBFNN 1 for joint 2 has 28 nodes and RBFNN 2 for joint 2 has 25 nodes. RBFNN 1 for joint 3 has 20 nodes and RBFNN 2 for joint 3 has 20 nodes. The central positions of the Gaussian functions c_i are selected from $[-1, 1]$ for all RBFNNs, and the spread factors are chosen to be $\sigma_i^1 = 0.2$

and $\sigma_i^2 = 0.2$ with i is the number of joints. $\delta_1^1 = 20, \delta_1^2 = 14$
 $\delta_2^1 = 20, \delta_2^2 = 14$ and $\delta_3^1 = 15, \delta_3^2 = 15$. In order to avoid the zero
 division if $\dot{e}_i(t) = 0$, the NNSTW controller (equation 19) is
 replaced by the super-twisting terminal sliding mode given
 by equation (17). The stability analysis and the RBFNNs
 parameters adjustment are detailed in the APPENDIX. A.
 Figures 4 and 5 present the simulation results of the
 application of the control laws (19) and (14). For every
 simulation, we present the angular position and the control
 signals. The NNSTW is presented by red lines and at the
 same time STW is presented by the blue lines. References
 are given by black lines.

$$\begin{aligned}
 q_{d1} &= \frac{\pi}{2000} t^3 - \frac{\pi}{400} t^2 & q_{d1}(0) &= 0 & q_{d1}(10) &= \frac{\pi}{4} \\
 q_{d2} &= \frac{\pi}{2000} t^3 - \frac{\pi}{400} t^2 & q_{d2}(0) &= 0 & q_{d2}(10) &= \frac{\pi}{4} \\
 q_{d3} &= \frac{\pi}{2000} t^3 - \frac{\pi}{400} t^2 & q_{d3}(0) &= 0 & q_{d3}(10) &= \frac{\pi}{4}
 \end{aligned}
 \tag{38}$$

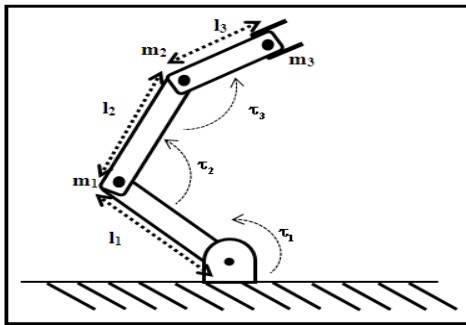


Fig. 3. 3-DOF robotic manipulator.

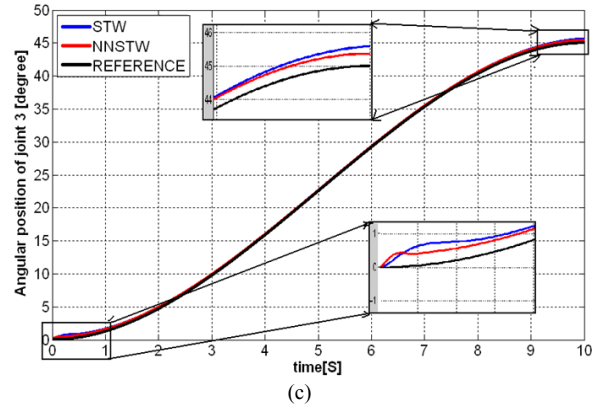
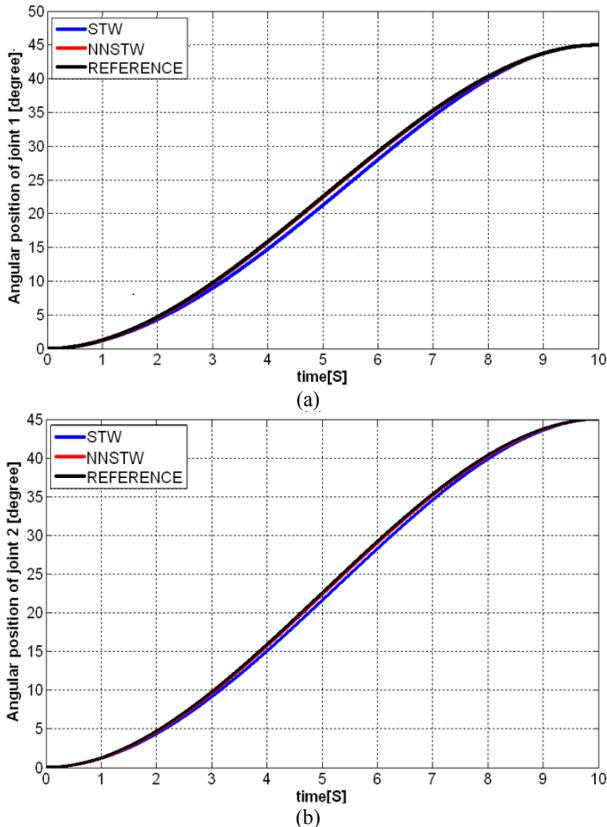


Fig. 4. Application of NNSTW and STW to all joints in trajectory tracking mode (a) joint 1 (b) joint 2 (c) joint 3.

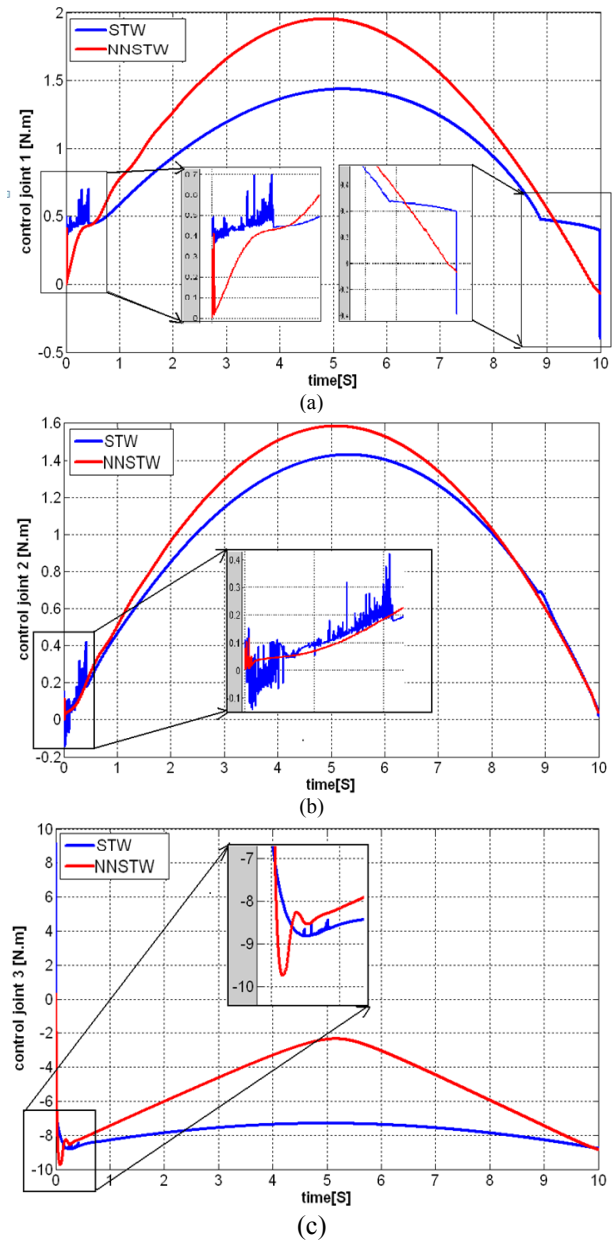


Fig. 5. Signals of the application of NNSTW and STW to all joints in trajectory tracking mode (a) joint 1, (b) joint 2 and (c) joint 3.

For all joints (figure 4 and 5) NNSTW presents better results compared with STW. This can be seen in the position responses for all joints, where, the maximal tracking errors in the case of STW are $(e_1, e_2, e_3) = (1.31, 0.98, -0.6)$ degrees for joints 1, 2 and 3 respectively. In the case of NNSTW the maximal tracking errors are equal to $(0.17, 0.23, -0.23)$ degrees for joints 1, 2 and 3 respectively. The control signals present a chattering in the beginning of the joints moves. In the case of the STW controller this behavior can be justified by two reasons; first, the joints coupling and; second, the friction forces. This justification can be confirmed in the control signal of joint 1 where between $t = 8.9$ s and 10 s is deviated. In the case of NNSTW, we have smooth control signals which are explained by the effect of the RBFNN; then, the chattering is moved in all trajectory tracking.

1. Robustness test:

The objective of this experience is to examine the robustness of the controllers by applying a permanent perturbation such as a mass load. We maintain the same desirable angles given by equation (38) and the experimental parameters are also the same. The used mass is equal to 0.2 kg. As in the above results (without mass load) Figures 6 and 7 present the results in trajectory tracking mode and the applied control signals for both approaches (STW and NNSTW).

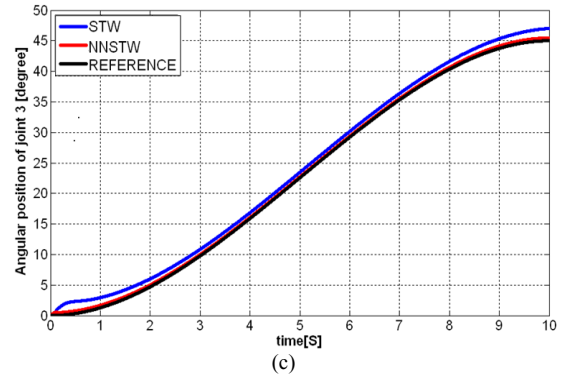
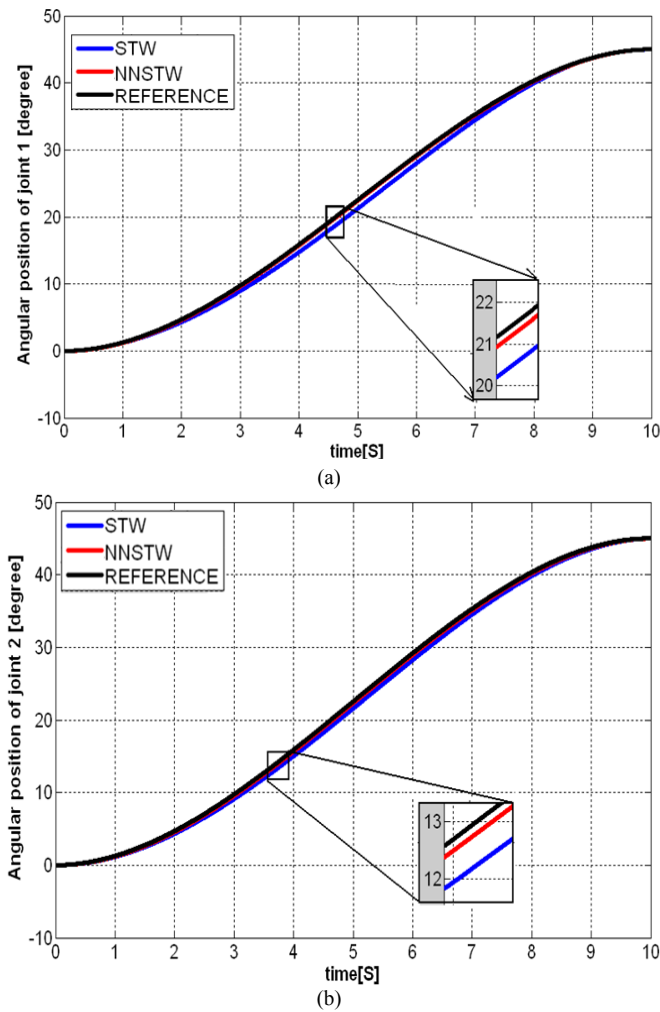


Fig. 6. Robustness tests of the incorporated mass load for the application of NNSTW and STW to all joints in trajectory tracking mode (a) joint 1, (b) joint 2 and (c) joint 3.

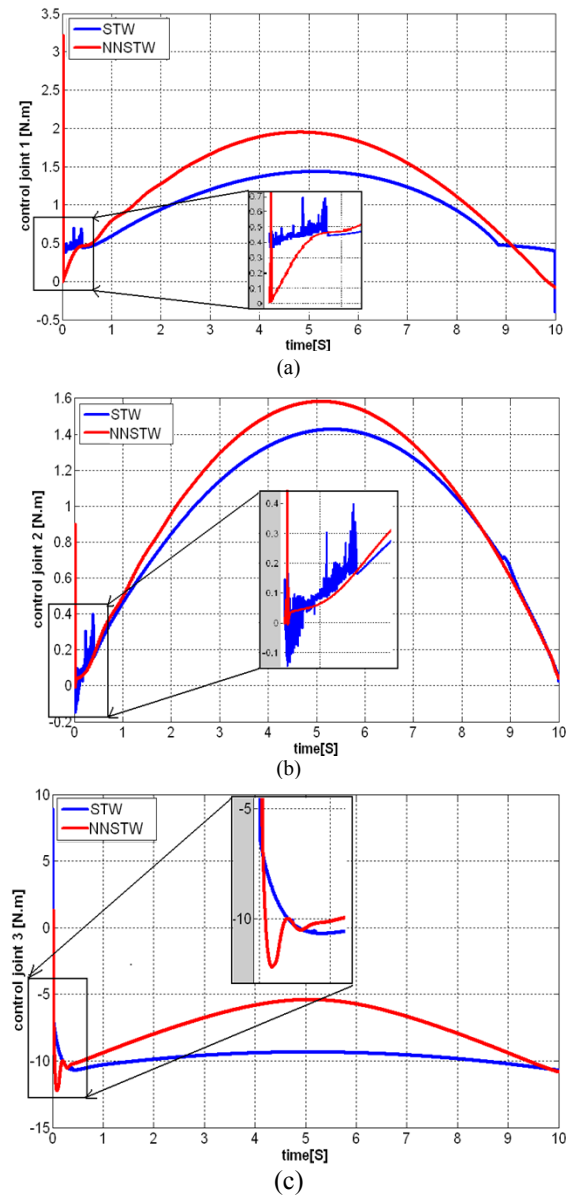


Fig. 7. control signals of the application of NNSTW and STW to all joints in trajectory tracking mode in presence of mass load (a) joint 1, (b) joint 2 and (c) joint 3.

The used mass load presents 28.47% of the mass of the joint 3. We can conclude from the angular response of joint 3 that the control based on the STW is not robust compared with the mass load uncertainty. The proposed NNSTW has presented good robustness and can overwhelm this uncertainty.

2. Quantitative performances comparison

A quantitative comparison is done here in order to analyze what is the better controller. We choose two criterions: the integral of absolute error (IAE) for evaluating the precision and the integral of absolute control (IA τ) to evaluate the consumed energy. These criterions are given by equations (39) and (40) and Figures 9 and 10 present the obtained results using these criterions.

$$IAE = \int_{t=0}^{t=t_f} |e| dt \tag{39}$$

$$IA\tau = \int_{t=0}^{t=t_f} |\tau| dt \tag{40}$$

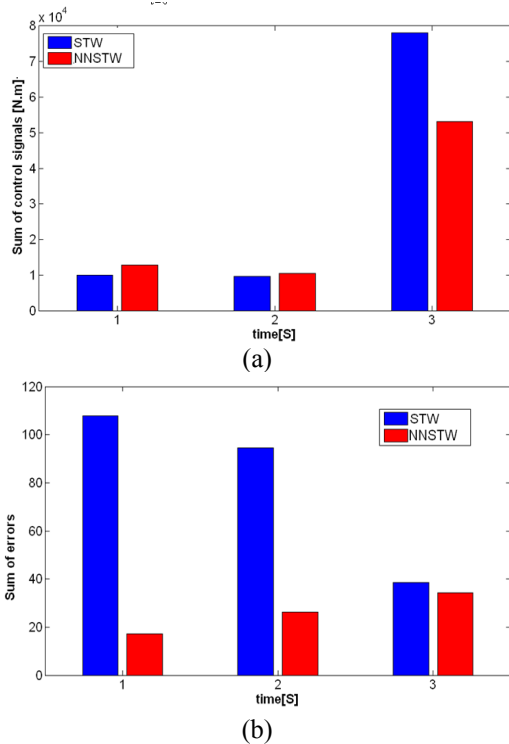


Fig. 9. Quantitative comparisons between STW and NNSTW (a) sum of absolute errors (b) sum of control torques.

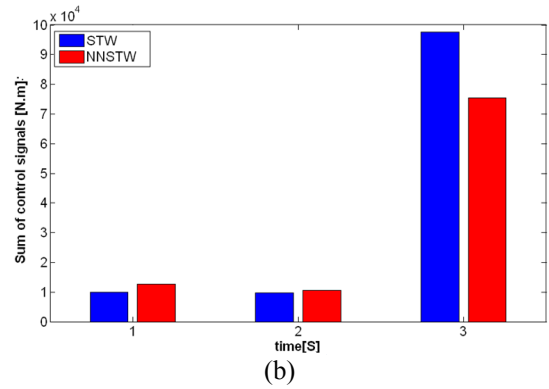
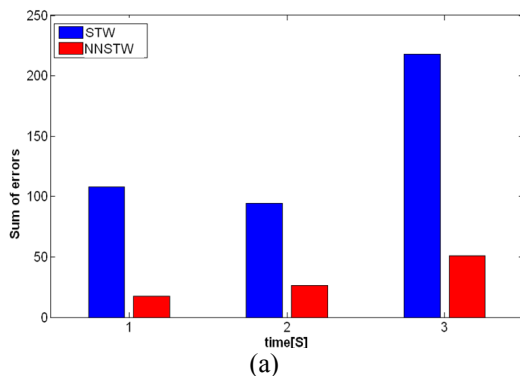


Fig. 10. Quantitative comparisons between STW and NNSTW (a) sum of absolute errors (b) sum of control torques.

All errors and consumed energy are reduced in the case of NNSTW compare with STW. We can conclude from the results shown in figure 9 and 10 that the NNSTW gives better results compared with the STW in presence of mass load uncertainty.

5. CONCLUSION

In this work, a new robust approach called Radial Based Function Neural Network Nonsingular Terminal Sliding Super Twisting Controller (NNSTW) is proposed for controlling *n*-DOF RM. The NTSMC with time delay estimation method is used to design the equivalent control without requirement of model knowledge. RBFNNs based on STW algorithm is proposed to remove the chattering phenomenon and to improve the control performance. The feasibility and the effectiveness of the proposed approach have been proven through simulation experiments. The proposed NNSTW presents better performance compared with the STW. Indeed, the control can be achieved without the robot model knowledge with improved performances and robustness.

REFERENCES

Astrom, K. J. and Hugglund, T. (1984). Automatic Tuning of Simple Regulators With Specifications on Phase And Amplitude Margins. Automatica. volume (20), issue (5) 645-651.

Bandyopadhyay, B. Janardhanan, S. and Spurgeon, S. K. (2013). Advances in Sliding Mode Control. Lecture Notes in Control and Information Sciences. Volume (440), Springer.

Cao, L. Chen, Y. Chen, X. Zhao, Y. and Fan, J. (2012). The Design and Analysis of Non-singular Terminal Adaptive Fuzzy Sliding-mode Controller. Proc. of the 2012 American Control Conference, 4625-4630, Canada.

Capisania, L. M. Ferrara, A. and Magnania, L. (2009). Design and Experimental Validation of a Second-Order Sliding-Mode Motion Controller for Robot Manipulator. Int. Journal of Control. Volume (82), Issue (2), 365-377.

Fei, J., H. Ding, S. Hou, Wang, S. and Xin, M. (2012). "Robust Adaptive Neural Sliding Mode Approach for Tracking Control of a MEMS Triaxial Gyroscope. Int J Adv Robotic Sy. Volume (9), 1-8.

- Fenga, Y. Yu, X. Manc Z. (2002). "Non-Singular Terminal Sliding Mode Control of Rigid Manipulators," *Automatica* Volume (38), Issue (2002), 2159 - 2167.
- Gokhan Ak A., and Cansever G. (2006), "Three Link Robot Control with Fuzzy Sliding Mode Controller Based on RBF Neural Network" *IEEE International Symposium on Intelligent Control, Germany*. PP. 2719-2724.
- Jia, T. and Kang, G. (2012). An RBF Neural Network-Based Nonsingular Terminal Sliding Mode Controller for Robot Manipulators. 3th Int. Conf. on Intelligent Control and Information Processing. 72 – 76, China.
- Jin, M. Lee, J. Chang, P. H. and Choi, C. (2009). Practical Nonsingular Terminal Sliding-Mode Control of Robot Manipulators for High-Accuracy Tracking Control. *IEEE Trans. On Industrial Electronics*. Volume (56), issue (9), 3593-3601.
- Jin, M. Jin, Y. Chang, P. H. and Choi, C. (2011). High-Accuracy Tracking Control of Robot Manipulators Using Time Delay Estimation and Terminal Sliding Mode. *Int. Journ al., Adv Robotic Sy.* Volume (8), issue (4), 65-78.
- Jin, Y. Chang, P. H. Maolin, J. and Gweon, D. G. (2013) Stability Guaranteed Time Delay Control of Manipulators Using Nonlinear Damping and Terminal Sliding Mode. *IEEE Trans. On Industrial Electronics*. Volume (60), Issue (8), 3304-3317.
- Islam, R. Iqbal, J. and Khan, Q. (2014). Design and Comparison of Two Control Strategies for Multi-DOF Articulated Robotic Arm Manipulator. *journal of control engineering and applied informatics*, Volume (16), issue (2), 28-39.
- Moldoveanu, F. Comnac, V. Floroian, D. Boldisor C. (2005), Trajectory Tracking Control Of a Two-Link Robot Manipulator Using Variable Structure System Theory, *journal of control engineering and applied informatics*, Volume (7), issue (3), 56-62.
- Kumar, N. Panwar, V. Borm, J.H. and Chai, J. (2014). Enhancing Precision Performance of Trajectory Tracking Controller for Robot Manipulators Using RBFNN and Adaptive Bound. *Applied Mathematics and Computation*. Volume (231), 320-328.
- Kuo, C. and Wang S., "Nonlinear robust industrial robot control," *J. Dyn. Syst., Meas., Contr.*, vol. 111, no. 1, pp. 24–30, 1989.
- Lei, X. Ge, S. S. and Fang, J. (2014). Adaptive Neural Network Control of Small Unmanned Aerial Rotorcraft. *J. Intell Robot Syst.* Volume (75), 331–341.
- Levant, A. (1993). Sliding Order And Sliding Accuracy In Sliding Mode Control. *Int. J. Control*, Volume (58), 1247-1263.
- Levant, A. (2003). Higher Order Sliding Modes, Differentiation and Output Feedback Control. *Int. J. Control*, Volume (76), Issue (9/10), 924-941.
- Lewis, F.L. Dawson, D.M. and Abdallah, C.T. (2004). *Robot Manipulator and Control -Theory and Practice*. Marcel Dekker. New York.
- Lian, R.J. (2011). Intelligent Controller for Robotic Motion Control. *IEEE Tran. On Industrials Electronics*. Volume (58), issue (11), 5220–5230.
- Lin, C. M. and Mon, Y. J. (2003). Hybrid Adaptive Fuzzy Controllers with Application to Robotic Systems. *Fuzzy Sets and Systems*. Volume (139), 151-165.
- Lin, C. K. (2006). Nonsingular Terminal Sliding Mode Control of Robot Manipulators Using Fuzzy Wavelet Networks. *IEEE Trans. On Fuzzy Systems*. Volume (14), issue (6), 849-859.
- Lu, H.C., Tsai, C.H., Chang, M.H., (2010). Radial Basis Function Neural Network with Sliding Mode Control for Robotic Manipulators. *IEEE Int. Conf. on Systems Man and Cybernetics*, 1209 – 1215. Turkey.
- Manceur, M. Essounbouli, N. and Hamzaoui, A. (2012). Second Order Sliding Fuzzy Interval Type-2 Control for an Uncertain System with Real Application. *IEEE Tran. On Fuzzy Systems*. Volume (20), issue (2), 262 - 275.
- Mondal, S. and Mahanta, C. (2014). Adaptive Second Order Terminal Sliding Mode Controller for Robotic Manipulators. *Journal of the Franklin Institute*. Volume (351), Issue (4), 2356-2377.
- Moradi M. and Malekizade, H. (2013). Neural Network Identification Based Multivariable Feedback Linearization Robust Control for a Two-Link Manipulator", *J Intell Robot Syst.* Volume (72),167-178.
- Perruquetti, W. and Barbot, J.P. (2002). *Sliding Mode Control in Engineering*. Marcel Dekker, New York.
- Qi, L. and Shi, H. (2013). Adaptive position tracking control of permanent magnet synchronous motor based on RBF fast terminal sliding mode control. *Neurocomputing*. Volume (115), 23–30.
- Rezoug, A. Mahjoub, S. Hamerlain, M. and Tadjine, M. (2011). Fuzzy Terminal Sliding Mode Controller for Robot Arm Actuated by Pneumatic Artificial Muscles. 8th Int. Multi-Conference on Systems, Signals and Devices, 22-25, Tunisia.
- Rezoug, A. Hamerlain, M. and Tadjine, M. (2012). Adaptive RBFNN type-2 fuzzy sliding mode controller for robot arm with pneumatic muscles. 2012 *IEEE Int. Conf. on Robotics and Biomimetics*. 1287-1292, Chine.
- Rezoug, A. Tondou, B. Hamerlain, M. and Tadjine, M. (2013). Adaptive Nonsingular Terminal Sliding Mode Control For Robot Manipulator Actuated By Pneumatic Artificial Muscles. 2013 *IEEE Int. Conf. on Robotics and Biomimetics*, 334 – 339, Chine.
- Sadati, N. Ghadami, R. (2008). Adaptive Multi-Model Sliding Mode Control of Robotic Manipulators Using Soft Computing. *Neurocomputing*. Volume (71), 2702-2710.
- Shtessel, Y. Edwards, C. Fridman, L. and Levant, A. (2014). *Sliding Mode Control and Observation*. Springer, New York.
- Song B. and Koivo A., "Nonlinear predictive control with application to manipulator with flexible forearm," *IEEE Trans. Ind. Electron.*, vol.46, no. 5, pp. 923–932, Oct. 1999.
- Tai, N. T., Ahn, K. K. 2010. A RBF Neural Network Sliding Mode Controller for SMA Actuator. *Int. Journal of Control, Automation, and Systems*. Volume (8), issue (6), 1296-1305.

Tang, Y. Sun, F. and Sun, Z. (2006). Neural Network Control of Flexible-Link Manipulators Using Sliding Mode. *Neurocomputing*. Volume (70), 288-295.

Van, M., Kang, H.J., Suh, Y.S. (2013). A Novel Fuzzy Second-Order Sliding Mode Observer- Controller for a T-S Fuzzy System With an Application for Robot Control. *Int. J. of Precision Engineering and Manufacturing*. Volume (14), issue (10), 1703-1711.

Youcef-Toumi, K. and Kondo, F. (1989) "Time delay control," in IEEE American Control Conference, 1989., pp. 1912-1917.

Pazelli, T. F., Terra, M. H. and Siqueira, A. A. (2011) "Experimental investigation on adaptive robust controller designs applied to a free-floating space manipulator," *Contr. Eng. Pract.*, vol. 19, no. 4, pp. 395-408.

APPENDIX A.

In the case of 3-DOF robot manipulator, the control law is given by equation (23) with $i=\{1,2,3\}$. In this case, we have four (4) RBFNNs, the general form of Lyapunov candidate in the case of 3-DOF robot manipulator $i=\{1,2,3\}$ is:

$$\begin{aligned} V &= \frac{1}{2} S^T S \\ &+ \frac{1}{2\delta_1^2} \tilde{W}_1^{1T} \tilde{W}_1^1 + \frac{1}{2\delta_1^2} \tilde{W}_1^{2T} \tilde{W}_1^2 + \frac{1}{2\delta_2^2} \tilde{W}_2^{1T} \tilde{W}_2^1 \\ &+ \frac{1}{2\delta_2^2} \tilde{W}_2^{2T} \tilde{W}_2^2 + \frac{1}{2\delta_3^2} \tilde{W}_3^{1T} \tilde{W}_3^1 + \frac{1}{2\delta_3^2} \tilde{W}_3^{2T} \tilde{W}_3^2 \end{aligned} \quad (41)$$

The time derivative of the Lyapunov function (36) is given as:

$$\begin{aligned} \dot{V} &= S^T \dot{S} \\ &+ \frac{1}{\delta_1^2} \tilde{W}_1^{1T} \dot{W}_1^1 + \frac{1}{\delta_1^2} \tilde{W}_1^{2T} \dot{W}_1^2 + \frac{1}{\delta_2^2} \tilde{W}_2^{1T} \dot{W}_2^1 \\ &+ \frac{1}{\delta_2^2} \tilde{W}_2^{2T} \dot{W}_2^2 + \frac{1}{\delta_3^2} \tilde{W}_3^{1T} \dot{W}_3^1 + \frac{1}{\delta_3^2} \tilde{W}_3^{2T} \dot{W}_3^2 \end{aligned} \quad (42)$$

Developing equation (42) as in equation (23), we have :

$$\begin{aligned} \dot{V} &= S^T \left[\dot{e} + \gamma \Lambda^{-1} \text{diag} \left(e^{\gamma-1} \right) \dot{e} \right] \\ &= S^T \left\{ \dot{e} + \gamma \Lambda \text{diag} \left(e^{-\gamma} \right) \right. \\ &\times \left. \left[-\gamma \Lambda^{-1} \dot{e}^{2-\gamma} \left(-\beta |S|^{1/2} \text{sign}(S) - \alpha \int_0^t \text{sign}(S(\tau)) d\tau + \varepsilon \right) \right] \right\} \\ &+ \frac{1}{\delta_1^2} \tilde{W}_1^{1T} \dot{W}_1^1 + \frac{1}{\delta_1^2} \tilde{W}_1^{2T} \dot{W}_1^2 + \frac{1}{\delta_2^2} \tilde{W}_2^{1T} \dot{W}_2^1 \\ &+ \frac{1}{\delta_2^2} \tilde{W}_2^{2T} \dot{W}_2^2 + \frac{1}{\delta_3^2} \tilde{W}_3^{1T} \dot{W}_3^1 + \frac{1}{\delta_3^2} \tilde{W}_3^{2T} \dot{W}_3^2 \end{aligned} \quad (43)$$

The time derivative of the sliding variables is given as:

$$\begin{aligned} \dot{S} &= \gamma \Lambda^{-1} \dot{e}^{2-\gamma} \left(-\beta |S|^{1/2} \text{sign}(S) - \alpha \int_0^t \text{sign}(S(\tau)) d\tau + \varepsilon \right) \\ &= \gamma \Lambda^{-1} \dot{e}^{\gamma-1} (\tilde{U} + \varepsilon) \end{aligned}$$

$$\begin{aligned} &= \gamma \Lambda^{-1} \dot{e}^{\gamma-1} \left(\begin{aligned} &\left[\begin{aligned} &|S_1|^{1/2} W_1^{1*} h_1^1(S) \text{Sign}(S_1) + W_1^{2T} h_1^2(S) \int_0^{t_{e1}} \text{Sign}(S_1) d\tau \\ &|S_2|^{1/2} W_2^{1T} h_2^1(S) \text{Sign}(S_2) + W_2^{2T} h_2^2(S) \int_0^{t_{e2}} \text{Sign}(S_2) d\tau \\ &|S_3|^{1/2} W_3^{1T} h_3^1(S) \text{Sign}(S_3) + W_3^{2T} h_3^2(S) \int_0^{t_{e3}} \text{Sign}(S_3) d\tau \end{aligned} \right] + \varepsilon \end{aligned} \right) \\ &= \gamma \Lambda^{-1} \dot{e}^{\gamma-1} \left(\begin{aligned} &\left[\begin{aligned} &|S_1|^{1/2} (W_1^1 - W_1^{1*})^T h_1^1(S) \text{Sign}(S_1) + (W_1^2 - W_1^{2*})^T h_1^2(S) \int_0^{t_{e1}} \text{Sign}(S_1) d\tau \\ &|S_2|^{1/2} (W_2^1 - W_2^{1*})^T h_2^1(S) \text{Sign}(S_2) + (W_2^2 - W_2^{2*})^T h_2^2(S) \int_0^{t_{e2}} \text{Sign}(S_2) d\tau \\ &|S_3|^{1/2} (W_3^1 - W_3^{1*})^T h_3^1(S) \text{Sign}(S_3) + (W_3^2 - W_3^{2*})^T h_3^2(S) \int_0^{t_{e3}} \text{Sign}(S_3) d\tau \end{aligned} \right] - \tilde{U}^* + \varepsilon \end{aligned} \right) \\ &= \gamma \Lambda^{-1} \dot{e}^{\gamma-1} \left(\begin{aligned} &\left[\begin{aligned} &|S_1|^{1/2} \tilde{W}_1^{1T} h_1^1(S) \text{Sign}(S_1) + \tilde{W}_1^{2T} h_1^2(S) \int_0^{t_{e1}} \text{Sign}(S_1) d\tau \\ &|S_2|^{1/2} \tilde{W}_2^{1T} h_2^1(S) \text{Sign}(S_2) + \tilde{W}_2^{2T} h_2^2(S) \int_0^{t_{e2}} \text{Sign}(S_2) d\tau \\ &|S_3|^{1/2} \tilde{W}_3^{1T} h_3^1(S) \text{Sign}(S_3) + \tilde{W}_3^{2T} h_3^2(S) \int_0^{t_{e3}} \text{Sign}(S_3) d\tau \end{aligned} \right] - \tilde{U}^* + \varepsilon \end{aligned} \right) \end{aligned} \quad (44)$$

Substituting the last equation of (44) in (42) yields:

$$\begin{aligned} \dot{V} &= S^T \left[\gamma \Lambda^{-1} \dot{e}^{\gamma-1} (-\tilde{U}^* + \varepsilon) \right] \\ &= S_1 \gamma \lambda_1^{-1} \dot{e}_1^{\gamma-1} (-\tilde{u}_1^* + \tilde{u}_1^*) + \varepsilon_1 \\ &+ S_2 \gamma \lambda_2^{-1} \dot{e}_2^{\gamma-1} (-\tilde{u}_2^* + \tilde{u}_2^*) + \varepsilon_2 \\ &+ S_2 \gamma \lambda_2^{-1} \dot{e}_2^{\gamma-1} (-\tilde{u}_3^* + \tilde{u}_3^*) + \varepsilon_2 \\ &= S_1 \gamma \lambda_1^{-1} \dot{e}_1^{\gamma-1} (-\alpha_1^* t_{e1} + \beta_1^* |S_1|^{1/2}) \text{sign}(S_1) + \varepsilon_1 \\ &+ S_2 \gamma \lambda_2^{-1} \dot{e}_2^{\gamma-1} (-\alpha_2^* t_{e2} + \beta_2^* |S_2|^{1/2}) \text{sign}(S_2) + \varepsilon_2 \\ &+ S_3 \gamma \lambda_3^{-1} \dot{e}_3^{\gamma-1} (-\alpha_3^* t_{e3} + \beta_3^* |S_3|^{1/2}) \text{sign}(S_3) + \varepsilon_3 \end{aligned} \quad (45)$$

If we have:

$$\begin{aligned} \alpha_1^* t_{e1} + \beta_1^* |S_1|^{1/2} &\geq \varepsilon_1 \\ \alpha_2^* t_{e2} + \beta_2^* |S_2|^{1/2} &\geq \varepsilon_2 \\ \alpha_3^* t_{e3} + \beta_3^* |S_3|^{1/2} &\geq \varepsilon_3 \end{aligned} \quad (46)$$

The time derivative of Lyapunov function is negative, consequently the stability of the controlled system is confirmed, and the adaptive RBFNNs parameters are given as:

$$\begin{aligned} \dot{W}_1^1 &= \gamma \delta_1^1 \lambda_1^{-1} \dot{e}_1^{\gamma-1} |S_1|^{3/2} h_1^1(S) \\ \dot{W}_1^2 &= \gamma \delta_1^2 \lambda_1^{-1} \dot{e}_1^{\gamma-1} h_1^2(S) \int_0^{t_{e1}} |S_1| d\tau \\ \dot{W}_2^1 &= \gamma \delta_2^1 \lambda_2^{-1} \dot{e}_2^{\gamma-1} |S_2|^{3/2} h_2^1(S) \\ \dot{W}_2^2 &= \gamma \delta_2^2 \lambda_2^{-1} \dot{e}_2^{\gamma-1} h_2^2(S) \int_0^{t_{e2}} |S_2| d\tau \\ \dot{W}_3^1 &= \gamma \delta_3^1 \lambda_3^{-1} \dot{e}_3^{\gamma-1} |S_3|^{3/2} h_3^1(S) \\ \dot{W}_3^2 &= \gamma \delta_3^2 \lambda_3^{-1} \dot{e}_3^{\gamma-1} h_3^2(S) \int_0^{t_{e3}} |S_3| d\tau \end{aligned} \quad (47)$$